Atmospheric photo-oxidation of acetic anhydride: kinetic study and reaction mechanism. Products distribution and fate of $CH_3C(O)OC(O)CH_2O\cdot$ radical

Jesús A. Vila[1,2], Guido N. Rimondino[1,3]*, Walter J. Peláez[1,3], Mateo Kalinowski[1], Fabio E. Malanca[1,3]

1) Departamento de Fisicoquímica, Facultad de Ciencias Químicas, Universidad Nacional de Córdoba, Ciudad Universitaria (X5000HUA), Córdoba, Argentina.

2) CICTERRA - CONICET/UNC - Centro de Investigaciones en Ciencias de la Tierra, Consejo Nacional de Investigaciones Científicas y Técnicas (X5016GCA) Córdoba, Argentina.

3) INFIQC - CONICET/UNC - Instituto de Investigaciones en Fisicoquímica de Córdoba, Consejo Nacional de Investigaciones Científicas y Técnicas (X5000HUA), Córdoba, Argentina.

***Corresponding author**

INFIQC – CONICET, Departamento de Fisicoquímica, Facultad de Ciencias Químicas, Universidad Nacional de Córdoba. Haya de la Torre s/n, Pabellón Argentina, ala oeste, segundo piso (X5000HUA) Ciudad Universitaria, Córdoba, Argentina.

e-mail address: grimondino@unc.edu.ar (G. N. Rimondino)

Abstract

The rate coefficient for the gas-phase reaction of acetic anhydride (Ac_2O) with chlorine atoms at 298 K and atmospheric pressure was experimentally determined ($k_{Ac2O+Cl}$ = (1.3 ± 0.4) × 10^{-12} cm^3 $molec^{-1}$ s^{-1}), while the rate coefficient for the reaction with the hydroxyl radical was estimated ($k_{Ac2O+OH}$ = 1.9 x 10^{-13} cm^3 $molec^{-1}$ s^{-1}). For the Structure-Activity Relationship method, a value of 0.02 was determined for the -C(O)OC(O) group. The mechanism of photo-oxidation of acetic anhydride initiated by chlorine atoms was determined and CO, CO_2, $CH_3C(O)OH$ (32 %), $CH_3C(O)OC(O)C(O)H$, and 3-hydroxy-1,4-dioxane-2,6-dione (20 %) were identified as products by infrared spectroscopy. Here we determined for the first time the relative energies of the primary reaction pathways for the $CH_3C(O)OC(O)CH_2O\cdot$ radical using computational methods, which confirmed our experimental data. Finally, the environmental implications of acetic anhydride emissions were calculated, showing an atmospheric lifetime between 31 and 220 days for the reaction with atmospheric radicals, while its wet deposition lifetime is 1.5 years.

Keywords

Rate coefficient, photo-oxidation, infrared spectroscopy, atmospheric lifetimes, Structure-Activity Relationship.

1 Introduction

Chemical reactions in the gas phase, more specifically the photo-oxidation reactions of volatile compounds in the environment lead to the formation of ozone and secondary organic aerosols, showing the importance of studying them. Although present in small concentrations, chlorine atoms play a significant role on tropospheric oxidation and can affect ozone production in urban environments. It is extremely reactive towards volatile organic compounds, with rate coefficients that are, with few exceptions, at least an order of magnitude greater than those of hydroxyl radicals (HO·), the key oxidant in the global atmosphere.(Calvert et al., 2011) In addition, Cl reacts rapidly with some compounds, with which HO· is relatively unreactive. Historically, Cl was thought to occur mainly in coastal areas and, consequently, the importance of Cl in atmospheric photo-oxidation processes was thought to be limited to the marine boundary layer.(Chang et al., 2004) However, other anthropogenic photolabile Cl precursors such as $ClNO_2$ and Cl_2 show the occurrence of different mechanisms for anthropogenic pollution to contribute to the photochemical production of Cl atoms in the atmosphere.(Young et al., 2014) Since these species can be found in continental areas, the potential impact of Cl on the tropospheric photo-oxidation chemistry of volatile organic compounds has been expanded.

Acetic anhydride (Ac_2O, $CH_3C(O)OC(O)CH_3$) is the simplest anhydride of a carboxylic acid. It is a colorless liquid with a characteristic pungent odor.(Cook, 1993) It is the largest commercially produced carboxylic acid anhydride with an approximate demand of 2,1 million tons in 2022 and with a view to grow.(Chemanalyst, 2023; Chemical Economics Handbook. S&P Global, 2023) It is widely used as a synthetic intermediate in organic synthesis, and as a solvent in certain analytical processes. However, its main industrial use is as an acetylating agent which reacts with nucleophiles to form acetic esters. Its major uses are in the manufacture of cellulose acetate fibers in the textile industry, or in the synthesis of aspirin and paracetamol in the pharmaceutical industry.(Wagner, 2014) It is also used in the plastics manufacturing and in the production of dyes, fragrances and even explosives. Its massive use on an industrial scale and its high volatility (4 mm Hg at 20°C) result in a considerable emission to the atmosphere that must be considered.(Lewis, 1997)

It is well known that anhydrides react rapidly in aqueous solution to form the two corresponding carbonyl acid compounds. In this sense, the degradation of Ac_2O in aqueous systems has been studied by several authors, as well its thermal decomposition.(Akao et al., 1996; Fritzler et al., 2014; Hirota et al., 2010; Knopp et al., 1962; Mai et al., 2017; Park and Lee, 2009) This fact may leave in the background the

study of the reactions of these compounds in the gas phase, assuming that they degrade easily in humid atmospheres, which is not the case, as will be shown in this work. That is why the study of its degradation in the gas phase has not been reported. Once Ac_2O is emitted to the atmosphere, its degradation mechanism could be initiated by HO· radicals or chlorine atoms, as shown in reactions 1 and 2, similar to other volatile organic compounds (Atkinson, 2007, 1997):

$$CH_3C(O)OC(O)CH_3 + HO\cdot \rightarrow CH_3C(O)OC(O)CH_2\cdot + H_2O \quad (1)$$

$$CH_3C(O)OC(O)CH_3 + Cl\cdot \rightarrow CH_3C(O)OC(O)CH_2\cdot + HCl \quad (2)$$

According to the symmetry of Ac_2O molecule, only $CH_3C(O)OC(O)CH_2\cdot$ radical could be formed. The presence of atmospheric oxygen leads to the formation of $CH_3C(O)OC(O)CH_2OO\cdot$ (reaction 3), which can subsequently react with another peroxy-radical or chlorine atom to give the corresponding oxy radical $CH_3C(O)OC(O)CH_2O\cdot$ (reaction 4 and 5).

$$CH_3C(O)OC(O)CH_2\cdot + O_2 \rightarrow CH_3C(O)OC(O)CH_2OO\cdot \quad (3)$$

$$2\ CH_3C(O)OC(O)CH_2OO\cdot \rightarrow 2\ CH_3C(O)OC(O)CH_2O\cdot + O_2 \quad (4)$$

$$CH_3C(O)OC(O)CH_2OO\cdot + Cl\cdot \rightarrow CH_3C(O)OC(O)CH_2O\cdot + ClO\cdot \quad (5)$$

Considering that the $CH_3C(O)OC(O)CH_2O\cdot$ radical is the only primary oxy radical formed by abstraction of a hydrogen from the molecule, Ac_2O is a good molecule to study the reaction pathways involving this radical, which is one of the objectives of this work. In addition, other aims of this work are the study of the rate coefficients of the reaction between Ac_2O and chlorine atoms, the determination of the atmospheric photooxidation products of Ac_2O and the postulation of the general reaction mechanism in the gas phase. Finally, the atmospheric lifetime resulting from the attack of the chlorine atom on the anhydride molecule was compared with that corresponding to wet deposition and an evaluation of the possible environmental consequences of Ac_2O emissions was presented.

2 Materials and methodology

Commercially available samples of Ac_2O (≥ 99%, Sigma), N_2 (5.5, Linde), O_2 (4.8, Praxair) acetone (HPLC, Sintorgan), ethyl acetate (HPLC, Sintorgan), formic acid (90%, Dorwil), and acetic acid (≥ 99%, Sigma Aldrich) were used as purchased. Cl_2 was obtained from the reaction between HCl and $KMnO_4$ and further distilled and stored in darkness.

The manipulation of gases was carried out in a passivated-glass vacuum line equipped with an absolute pressure transducer (0 to 760 Torr, MKS Baratron). All experiments were performed in a glass photo-reactor (volume = 3.6 L; optical path = 23 cm) equipped with KBr windows, which was placed in the Fourier Transform Infrared (FTIR) spectrometer (Bruker IFS-28) path and connected to the vacuum line. The temporal variation on the concentration of samples was monitored using infrared spectroscopy. Spectra were acquired every 40 seconds in the range 3000 - 500 cm^{-1} with a resolution of 2 cm^{-1}.

Ac_2O (10 μL) was injected in the photo-reactor through a Teflon septum. For the determination of the rate coefficients, 1.2 mbar of Cl_2 and 1013 mbar N_2 were added, while for the photooxidation experiments nitrogen were replaced O_2. All experiments were carried out at 298 K and atmospheric pressure. Photolysis of chlorine molecule was performed using by two black lamps (Phillips, 8 W, 350 nm < λ < 400 nm). To check the absence of heterogeneous reactions that may occur in the dark, similar experiments were carried out using the same gas mixture (Ac_2O, Cl_2, and N_2 or O_2) in the absence of irradiation.

The relative method (Atkinson, 1986) was used to determine the rate coefficient of the reaction between Ac_2O and chlorine atoms, $k_{Ac2O+Cl}$ (reaction 2), comparing the time variation of its concentration with two reference compounds whose rate coefficients with chlorine atoms are well known: acetone and ethyl acetate (reactions 6 and 7, respectively).

$$CH_3C(O)CH_3 + Cl\cdot \rightarrow \text{Products} \quad (6)$$

$$CH_3C(O)OCH_2CH_3 + Cl\cdot \rightarrow \text{Products} \quad (7)$$

From the analysis of the results, Equation 1 is derived and was used to determine the rate coefficient of the reaction between Ac_2O and chlorine atoms:

$$ln\left(\frac{[Ac_2O]_0}{[Ac_2O]_t}\right) = \frac{k_{Ac_2O+Cl}}{k_{Ref+Cl}} . ln\left(\frac{[Ref]_0}{[Ref]_t}\right) \quad \text{(Equation 1)}$$

where, $[Ac_2O]_0$, $[Ref]_0$, $[Ac_2O]_t$, and $[Ref]_t$ correspond to the acetic anhydride and reference compounds concentrations before and at different irradiation times, respectively; $k_{Ac2O+Cl}$ and k_{Ref+Cl} are the rate coefficients corresponding to the acetic anhydride and the reference compound with chlorine atom, respectively.

To estimate a rate coefficient of the reaction between Ac_2O and OH radicals, a correlation between the rate coefficients values (k_{Ref+OH} and k_{Ref+Cl}) reported in the literature for a series of carbo-oxygenated compounds (ketones and esters) was used to estimate the value of $k_{Ac2O+OH}$. From the free energy graph and the linear regression, the

149 $k_{Ac2O+OH}$ value was extrapolated from the experimental $k_{Ac2O+Cl}$ value.

150 Quantum chemical calculations using the DFT level of theory (B3LYP/6-
151 311+G(d,p) functional, Gaussian16 Program system)(Frisch et al., 2009) have been
152 carried out in order to investigate the primary paths for the reaction of alkoxy radical
153 $CH_3C(O)OC(O)CH_2O\cdot$. To determine the energies of the stable stationary points in the
154 potential energy surfaces, harmonic frequency calculations for the different possibles
155 intermediaries were calculated, similarly to recent works.(Rimondino et al., 2023,
156 2021, 2020)

157 Theoretical infrared spectra were calculated to perform the identification of the
158 unknown products formed during photooxidation. First, the conformational study of
159 the possible expected products was performed, from which their theoretical infrared
160 spectra were obtained using the Gaussian16 Program, and the frequency corresponding
161 to each peak was corrected according to equation 2 (Yoshida et al., 2002):

162 $$\frac{v_{exp}}{v_{calc}} = 1.00 - 0.0000105 * v_{calc} \qquad \text{(Equation 2)}$$

163 were ν_{exp} and ν_{calc} correspond to the experimental and theoretical wavenumbers,
164 respectively.

165

166 **3 Results and discussion**

167 **3.1 Kinetic studies**

168 Kinetic studies of the reaction between Ac_2O and chlorine atoms (reaction 2)
169 were determined from the relative method (Atkinson, 1986) using acetone and ethyl
170 acetate as reference compounds. The experiments were performed during irradiation
171 periods of less than 15 minutes. During this period, the decomposition of acetic
172 anhydride as consequence of heterogeneous or non-photolytic reactions was negligible
173 (less than 1.0 %). From each data set, $\ln([Ac_2O]_o/[Ac_2O]_t)$ *vs.* $\ln([Ref]_o/[Ref]_t)$ was
174 plotted and the values of the corresponding slopes, which correspond to $k_{Ac2O+Cl}/k_{Ref+Cl}$,
175 were obtained. From the values reported in the literature and least squares fits, values
176 of the rate constant for the reaction of Ac_2O with chlorine atoms were derived. Figure 1
177 shows the kinetics results using two references compounds: acetone and ethyl acetate.
178 Table 1 summarizes the values obtained in each experiment.

179

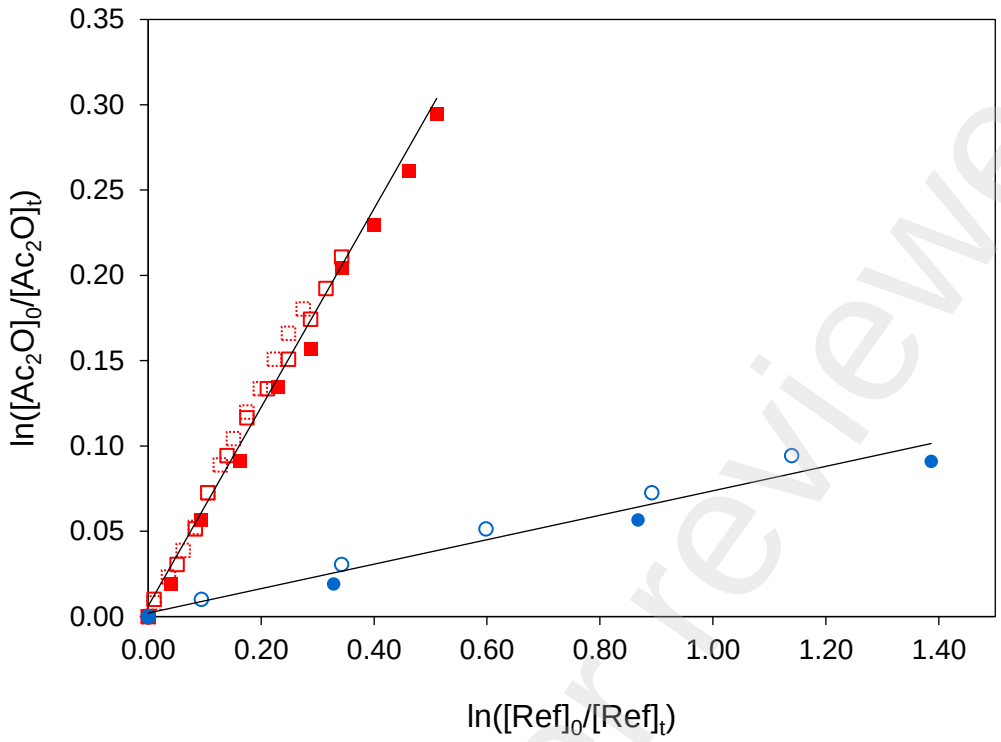

Figure 1. *Plot of kinetic data obtained using acetone (open, filled, and dotted red circles) and ethyl acetate (open and filled blue squares) as reference compounds at 298 K and 1 atm total pressure. The black lines correspond to the linear fit of the experimental points for each of the reference compounds.*

Reference compound	k_{Ref+Cl} ($\times 10^{12}$ cm^3 molec^{-1} s^{-1})	Slopes	Mean value slopes	$k_{Ac2O+Cl}$ ($\times 10^{12}$ cm^3 molec^{-1} s^{-1})
Acetone	(2.1 ± 0.3)	0.57 0.67 0.61	0.62 ± 0.05	1.3 ± 0.3
Ethyl acetate	(18.5 ± 3.5)	0.081 0.065	0.073 ± 0.011	1.4 ± 0.5

Table 1. *Experimental parameters for the reaction of Ac_2O with chlorine atoms using acetone and ethyl acetate as reference compounds. The error associated with the mean value of $k_{Ac2O+Cl}$ corresponds to a standard deviation.*

The rate coefficient for the reaction of Cl atoms with each reference presented in Table 1 were taken from bibliography (Notario et al., 1998). As can be seeing, the rate coefficient values obtained for the reaction of Ac_2O with Cl atoms using both reference compounds show good agreement with each other, validating the results. From those, and considering that the error was calculated as 2σ, a mean value of $k_{Ac2O+Cl}$ = (1.3 ±

196 0.4) × 10^{-12} cm^3 $molec^{-1}$ s^{-1} was derived.

197 The rate coefficient of the reaction of Ac_2O with OH radicals, $k_{Ac2O+OH}$, were also
198 evaluated. In this case, the irradiation times required to reach significant conversion
199 percentages were higher than 40 minutes, resulting in the occurrence of heterogeneous
200 reactions for Ac_2O in a percentage higher than 8 %, which introduces a considerable
201 error. For this reason, it was obtained an estimated value for $k_{Ac2O+OH}$ from a correlation
202 between the reported values of k_{OH} and k_{Cl}, as is used by other authors.(Scollard et al.,
203 1993; Straccia C et al., 2023) Given the presence of carbonyl groups in the Ac_2O
204 structure, other carbo-oxygenated molecules such as ketones and esters were used to
205 construct the graph. Figure 2 shows the plot of -log(k_{OH}) *vs.* -log(k_{Cl}) for the following
206 species: acetone, 2-butanone, 2-pentanone, 3-pentanone, 3-methylbutanone, 2-
207 hexanone, 3-hexanone, cyclopentanone, cyclohexanone, methyl formate, ethyl formate,
208 *n*-propyl formate, *n*-butyl formate, *t*-butyl formate, methyl acetate, ethyl acetate, *n*-
209 propyl acetate, *n*-butyl acetate, isobutyl acetate, methyl propionate, methyl *n*-butyrate,
210 and methyl *n*-pentanoate. Kinetics values for all these molecules were obtained from
211 those recommended by Calvert et al. (2011).

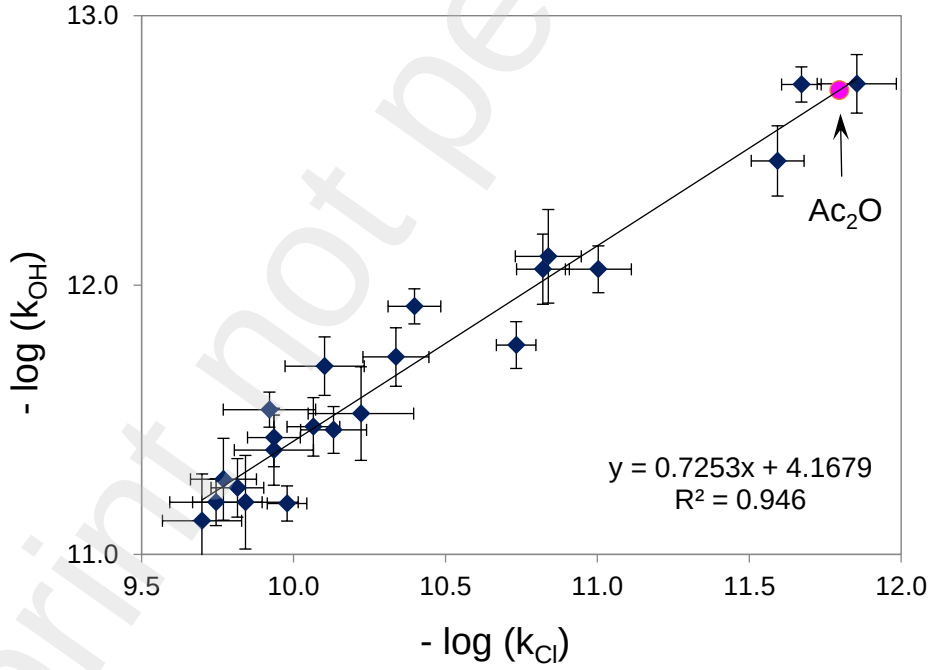

212

213 **Figure 2.** *Free-energy plot for a series of carbo-oxygenated molecules at*
214 *298 K. The magenta circle corresponds to the relationship obtained graphically for*
215 *Ac_2O.*

216

As can be seen in the plot, there is an excellent correlation between the kinetic parameters obtained for the reactions of these species with chlorine atoms and the reactions with OH radicals. From this, and employing the linear regression parameters of these data, the $k_{Ac2O+OH}$ value was extrapolated from the experimentally obtained rate coefficient with chlorine atoms presented above. From here, a value of (1.90 ± 0.3) × 10^{-13} cm^3 $molec^{-1}$ s^{-1} was derived.

3.2 SAR (Structure-Activity Relationship)

The SAR method allows estimating a value of the rate coefficient from the structure of the molecule, considering the abstraction of a hydrogen atom from each of the alkyl groups it contains, taking into account that its reactivity is modified by the substituents attached to each of these alkyl groups.(Atkinson, 1987; Kwok and Atkinson, 1995) According to this method, the estimation for Ac_2O was calculated as follows:

$$k_{Ac2O} = 2 \times [k_{prim} \times F(\text{-C(O)OC(O)})] \quad \text{(Equation 3)}$$

Using the value for k_{prim} = 3.32 × 10^{-11} cm^3 $molec^{-1}$ s^{-1} determined by (Atkinson, 1987; Kwok and Atkinson, 1995), a value of F(-C(O)OC(O)) = 0.020 was determined. This value is lower than the determined for F(-C(O)) = 0.04 (Notario et al., 1998), suggesting a deactivating effect of the anhydride group on the adjacent alkyl group, that is almost twice as great as if only the carbonyl were considered.

3.3 Photo-oxidation studies

To analyze the evolution of photo-oxidation products, mixtures containing Ac_2O (10 µL), Cl_2 (1.2 mbar) and O_2 (1013 mbar) were photolyzed at 298 K. Figure 3 shows the experimental infrared spectra obtained after two irradiation times and reference spectra, which were used for the analysis of the products generated. The first and second traces (traces A and B, respectively) correspond to the spectra obtained at photolysis times of 0 and 10 minutes, respectively. The third trace (trace C) was obtained from the digital subtraction of the signals corresponding to unreacted Ac_2O from trace B (focusing on the disappearance of the band around 1136 cm^{-1}). Trace C, thus, contains the infrared pattern of to the photo-oxidation products of Ac_2O. At the glance, the characteristic bands corresponding to the presence of HCl, CO, CO_2 are observed. Further, the comparison of trace C also shows signals at around 1800 and 1180 cm^{-1}, which correspond to the presence of acetic acid ($CH_3C(O)OH$) as a

degradation product of Ac_2O. For comparison purposes, the reference spectrum of $CH_3C(O)OH$ is shown on trace D.

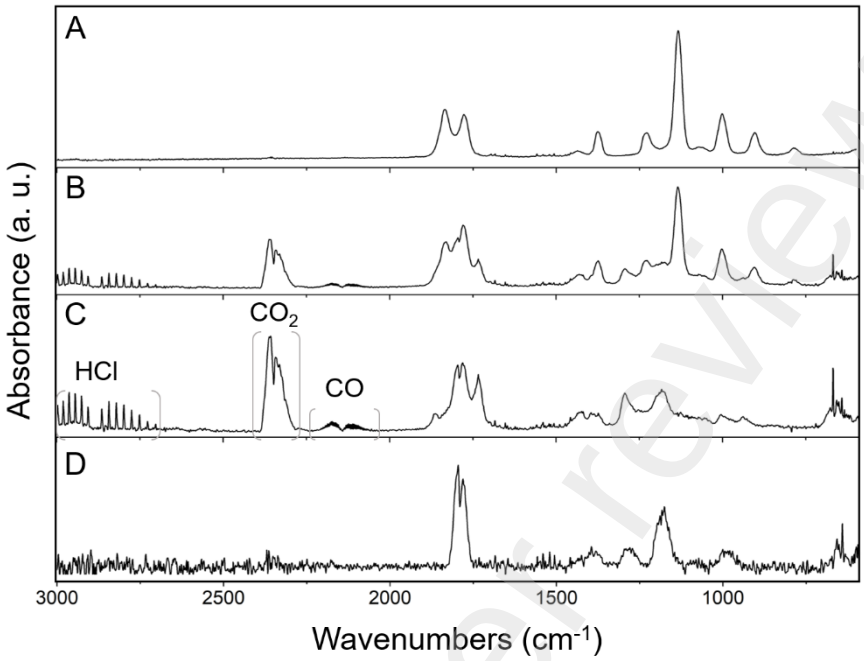

Figure 3. *Spectra obtained during the photo-oxidation of Ac_2O. Trace A corresponds to the mixture of reactants, trace B shows the spectrum obtained after 10 min of photolysis, trace C shows the photolysis products, and trace D show the reference spectrum of $CH_3C(O)OH$.*

Figure 4 presents the identification of the remaining products. The upper trace corresponds to the infrared spectrum obtained after subtraction of CO, CO_2, HCl, and $CH_3C(O)OH$ from trace "C" in Figure 4 and reveals the formation of additional products. To assign these identities, the theoretical spectra of the possible photooxidation products (as will be described in the reaction mechanism) were calculated by DFT methods. According to the possible reaction pathways that could be carried out, theoretical spectra were calculated for the proposed products. In particular, it can be observed that the spectra obtained for products 3-hydroxy-1,4-dioxane-2,6-dione (hereafter named as “cyclic anhydride”) and acetic 2-oxoacetic anhydride ($CH_3C(O)OC(O)C(O)H$, hereafter referred as “tricarboxylic aldehyde”) (second and third traces, respectively) show a good correspondence both in band position and their relative intensities with the obtained experimental spectra. Therefore, the formation of these compounds is established as products of photo-oxidative degradation.

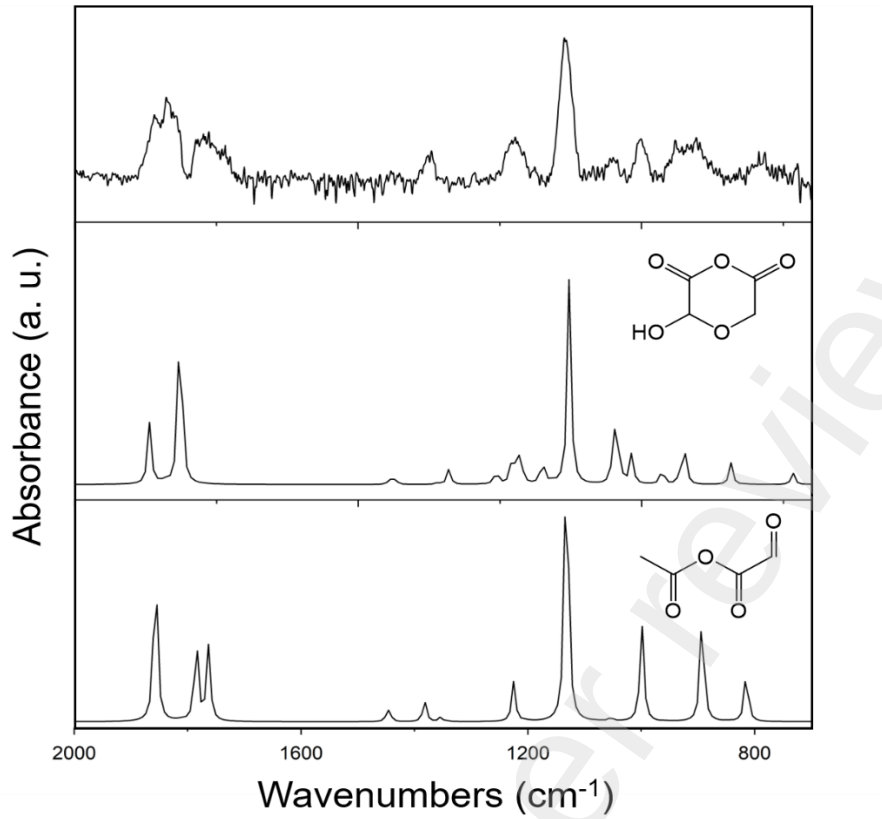

Figure 4. *Comparison of the residual spectrum of photooxidation products of Ac_2O (upper trace) with theoretical spectra of the cyclic anhydride (middle trace) and the tricarboxylic aldehyde (lower trace).*

Once the identity of the products was determined, they were quantified to establish the incidence of each Ac_2O degradation pathway. The temporal variation of CO_2, CO and $CH_3C(O)OH$ during the irradiation period (720 s) was performed using calibration curves obtained under the same experimental conditions. Once these products were quantified, the relative percentage of each product was calculated as a function of the amount of Ac_2O consumed at each time. In this way, the percentage ratio of each product as a function of the reaction time was obtained, as shown in Figure 5.

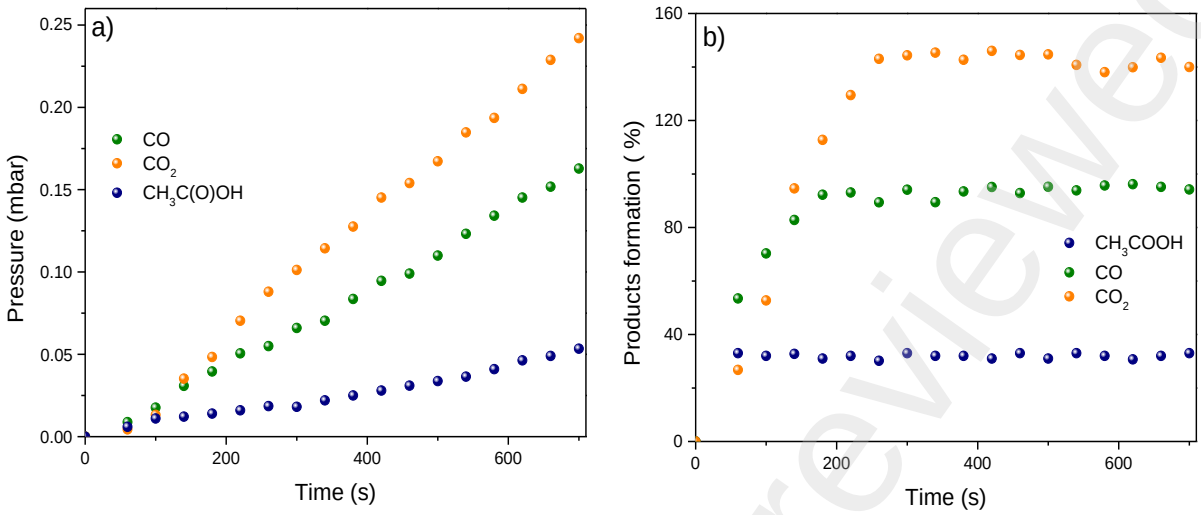

285

286 ***Figure 5.*** *a) Temporal variation of the amount (pressure) of the photo-*
287 *oxidation products, and b) temporal variation of their percentage of formation.*

288

289 The results indicate that the percentage of $CH_3C(O)OH$ formation is constant
290 (32%) during all the photolysis time. On the other hand, the percentage of CO gradually
291 increases from 0 to 250 seconds and then remains constant (94 %). A similar behavior
292 can be observed for the percentage of CO_2, which increases up to about 143% and then
293 remains constant. These results clearly demonstrate that acetic acid is a primary
294 product, while CO and CO_2 are secondary products, as will be shown in the discussion
295 of the photooxidation mechanism.

296 The stability of the products in the system was studied for a period of 2 hours in
297 the dark after switching off the photolysis lamps. The spectra obtained reveal that the
298 signals corresponding to the cyclic anhydride decrease while simultaneously the signals
299 of formic acid increase. This trend is maintained until the complete disappearance of
300 the cyclic anhydride, at which time the increase in HC(O)OH concentration no longer
301 changes. This result allows inferring that the formation of formic acid from the cyclic
302 anhydride is a consequence of heterogeneous decomposition against the reactor walls.
303 The maximum amount of HC(O)OH reached in the system corresponds to 20 % with
304 respect to the disappearance of acetic anhydride. Moreover, the appearance of formic
305 acid as a product confirms the presence of a fragment which have a carbon atom
306 bonded to both, an hydroxylic group and another oxygen atom (Rimondino et al., 2021,
307 2020), which is in accordance with the structure of the product presented in Figure 4.
308 In contrast, the signals corresponding to the tricarboxylic aldehyde

309 $CH_3C(O)OC(O)C(O)H$ do not change during the dark period, indicating that this
310 product is relatively stable under these conditions. Furthermore, this demonstrates that
311 formic acid is formed exclusively from the heterogeneous decomposition of the cyclic
312 anhydride.

313

314 **3.4 Reaction mechanism**

315 As mentioned previously, the photooxidation of Ac_2O is initiated by the attack of
316 a chlorine atom to the CH_3 group of the molecule, leading to the formation of the
317 $CH_3C(O)OC(O)CH_2\cdot$ radical (reaction 2). This reacts with oxygen to form the peroxy-
318 radical (reaction 3) and its subsequent reaction with the chlorine atom or another
319 peroxy-radical to form the oxy radical $CH_3C(O)OC(O)CH_2O\cdot$ (reactions 4 and 5,
320 respectively). According to the structure of the oxy-radical, it could, *a priori,* evolve in
321 four ways: react with molecular oxygen (*A*), rupture (*B*), rearrange (*C*), or isomerize (*D*)
322 (Orlando et al., 2003).

323 To determine the relative importance of each primary reaction route of
324 $CH_3C(O)OC(O)CH_2O\cdot$ mentioned above, a theoretical study was performed using
325 quantum mechanical calculations. First, a conformational search was performed at
326 B3LYP/6-311+G(d,p) level. Figure 6 shows the potential energy surface plot (PES),
327 where the global minimum corresponds to a structure where the oxygen of the carbonyl
328 group and the alkoxy moiety are outside the plane that contains the anhydride
329 fragment (Figure 6, right panel). Later, full geometry optimization of the most stable
330 conformer for the oxy-radical was performed.

331

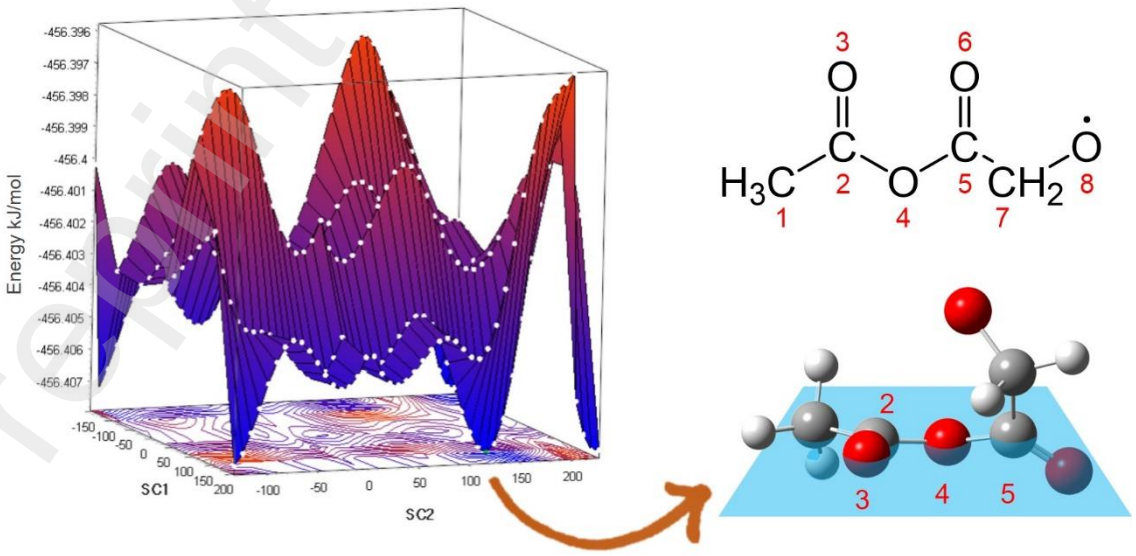

332

Figure 6. *PES B3LYP/6-311+G(d,p) and most stable conformer of oxy-radical of Ac_2O.*

Starting from the most stable conformer of the oxy-radical, computational studies were carried out to determine the relative energies for each proposed reaction coordinate, as well as the corresponding transition states and products for each path. The nature of the stationary points was determined by frequency calculations. Figure 7 shows the change of Gibbs Energy for the reaction coordinate for these *vias*.

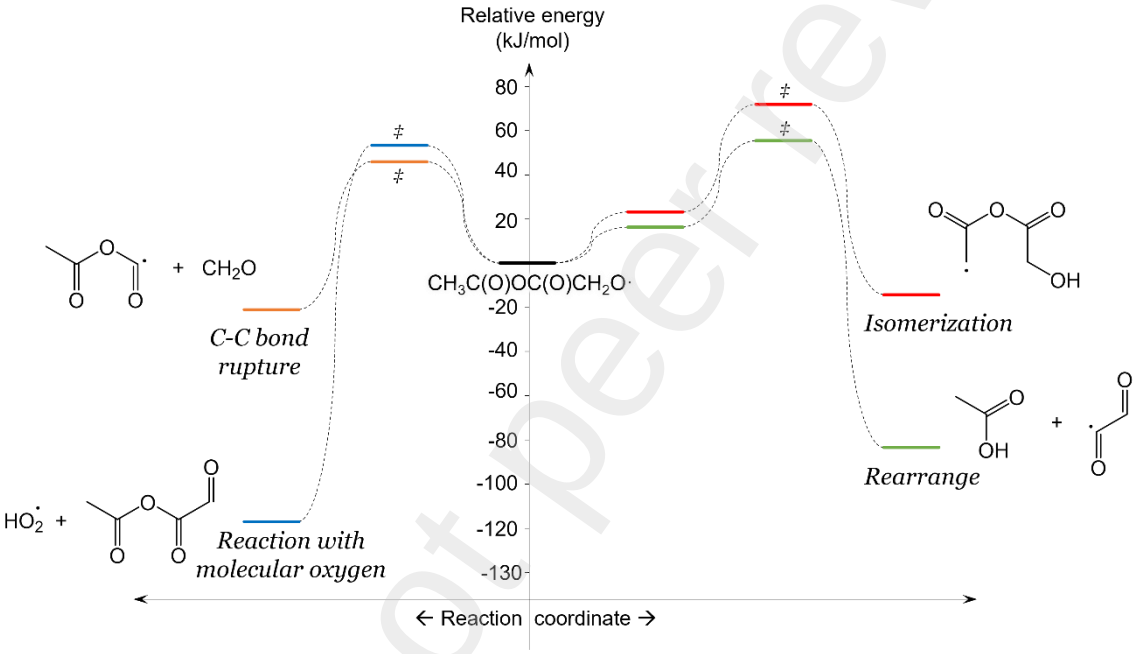

Figure 7. *Reaction coordinates for each primary path and formed products. The energy of the $CH_3C(O)OC(O)CH_2O\cdot$ radical was set at 0 kJ/mol.*

As can be seen, the abstraction of a hydrogen atom by molecular oxygen (hereafter named as *via A*) requires 53.57 kJ/mol to occur and it is exothermic around -117 kJ/mol. The C-C fragmentation path of the oxy-radical to give formaldehyde and a new radical (*via B*) is the most energetically favorable and require 45.99 kJ/mol and it is exothermic, reaching -21,29 kJ/mol. *Vias C* and *D* involving the rearrangement or isomerization of radical, respectively, occurs both in two consecutive steps. In a first stage, the oxy-radical take the most favored configuration to reach the transition states that will give rise to the final reaction products of each pathway, from where the H-migration or H-abstraction process occur. For the H-migration or process (*via C*) any of the two H-atoms from the methylene to the carbonyl of the acetyl group can generate

356 acetic acid and the HC(O)C(O)· radical. In this case, the energy difference to reach the
357 products was calculated for the two methylene protons of the alkoxy moiety and the
358 results showed a negligible difference (0.16 kJ/mol). On the other hand, in the
359 isomerization path (*via D*), it is the alkoxy group that abstracts one of the three
360 equivalent H-atoms from the methyl of the acetyl group. Calculations shows that this
361 pathway is the most energetically unfavorable (72.51 kJ/mol).

362 Once the energy parameters involved have been calculated and the possibility
363 that all the proposed *vias* are energetically favorable has been evaluated, the detailed
364 sequence of the degradation pathways of the oxy-radical $CH_3C(O)OC(O)CH_2O\cdot$ are
365 presented in Scheme 1.

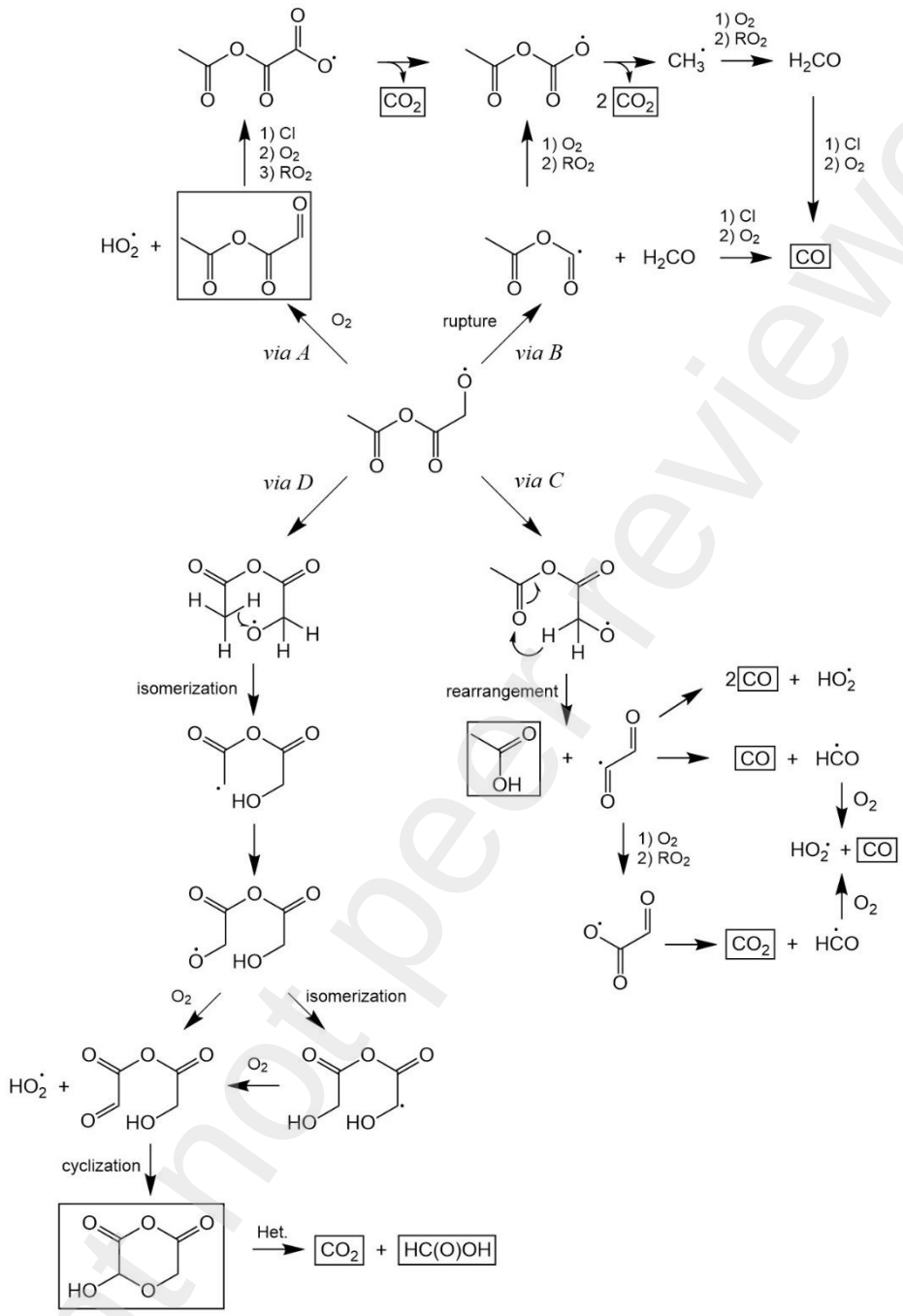

Scheme 1*. Reactions path for $CH_3C(O)OC(O)CH_2O\cdot$ radical. Squares remarks the observed products.*

The triggered reactions lead to final the formation of CO, CO_2, $CH_3C(O)OH$, the cyclic anhydride, and the tricarboxylic aldehyde. All these products were observed during the photo-oxidation as was presented in Figures 3 and 4. As mentioned previously, the last product leads to the formation of formic acid, therefore it was included as final product in the mechanism reaction.

A detailed analysis of the reactions of each pathway is presented below.

Via A

Oxy radicals (RO·) react with O_2 to form the correspondent aldehyde and HO_2· radicals (Orlando et al., 2003). For $CH_3C(O)OC(O)CH_2O$·, this path leads to the formation of the tricarboxylic aldehyde $CH_3C(O)OC(O)C(O)H$ (reaction 8), which was identify as a photo-oxidation product.

$$CH_3C(O)OC(O)CH_2O\cdot + O_2 \rightarrow CH_3C(O)OC(O)C(O)H + HO_2\cdot \quad (8)$$

Tricarboxylic aldehyde, $CH_3C(O)OC(O)C(O)H$, could react with chlorine atoms present in the system. As it is well known, for acetaldehyde, this reaction has a relatively high-rate coefficient: 8.0×10^{-11} cm^3 $molecule^{-1}$ s^{-1}.(Calvert et al., 2011). Considering the $CH_3C(O)OC(O)C(O)H$ has the same number of hydrogen atoms and similar structure that acetaldehyde, the attack of chlorine atoms should occur as shown reaction 9:

$$CH_3C(O)OC(O)C(O)H + Cl\cdot \rightarrow CH_3C(O)OC(O)C(O)\cdot + HCl \quad (9)$$

The radical $CH_3C(O)OC(O)C(O)$· could further react with O_2 leading to the formation of the peroxy-radical $CH_3C(O)OC(O)C(O)OO$· (reaction 10):

$$CH_3C(O)OC(O)C(O)\cdot + O_2 \rightarrow CH_3C(O)OC(O)C(O)OO\cdot \quad (10)$$

followed by reactions 11 and/or 12:

$$CH_3C(O)OC(O)C(O)OO\cdot + Cl\cdot \rightarrow CH_3C(O)OC(O)C(O)O\cdot + ClO\cdot \quad (11)$$

$$2\ CH_3C(O)OC(O)C(O)OO\cdot \rightarrow 2\ CH_3C(O)OC(O)C(O)O\cdot + O_2 \quad (12)$$

Produced $CH_3C(O)OC(O)C(O)O$· undergoes through successive decarboxylation steps (reaction 13 and 14):

$$CH_3C(O)OC(O)C(O)O\cdot \rightarrow CH_3C(O)OC(O)\cdot + CO_2 \quad (13)$$

Similar sequence of reactions for $CH_3C(O)OC(O)$· with molecular oxygen and then with chlorine atoms or other peroxy-radicals leads finally to the formation of a third CO_2 and CH_3· radicals, which in turn leads to the formation of H_2CO as shown reactions 14 to 17:

$$CH_3\cdot + O_2 \rightarrow CH_3O_2\cdot \quad (14)$$

$$2\ CH_3O_2\cdot \rightarrow 2\ CH_3O\cdot + O_2 \quad (15)$$

$$CH_3O_2\cdot + Cl\cdot \rightarrow CH_3O\cdot + ClO\cdot \quad (16)$$

$$CH_3O\cdot + O_2 \rightarrow H_2CO + HO_2\cdot \quad (17)$$

The presence of formaldehyde was not observed in our system, probably as a consequence of its high reactivity with chlorine atoms (7.0×10^{-11} cm^3 $molecule^{-1}$ s^{-1}).(Calvert et al., 2011) The rate coefficient for H_2CO is almost an order of magnitude greater than that found for the acetic anhydride (1.6×10^{-12} cm^3 $molecule^{-1}$ s^{-1}, this work), and therefore disappear more rapidly than the anhydride. Photo-oxidation of formaldehyde leads finally to the formation of CO, which was observed:

$$H_2CO + Cl\cdot \rightarrow HCO\cdot + HCl \quad (18)$$

$$HCO\cdot + O_2 \rightarrow CO + HO_2\cdot \quad (19)$$

Via B

The C-C bond rupture of $CH_3C(O)OC(O)CH_2O\cdot$ give the formation of formaldehyde and $CH_3C(O)OC(O)\cdot$ (reaction 20):

$$CH_3C(O)OC(O)CH_2O\cdot \rightarrow CH_3C(O)OC(O)\cdot + H_2CO \quad (20)$$

As was discussed in *via* A, the chemistry of $CH_3C(O)OC(O)\cdot$ and H_2CO leads finally CO and CO_2.

Via C

This path corresponds to an intramolecular 1,5-hydrogen shift to form $CH_3C(O)OH$ and $HC(O)C(O)\cdot$.

$$CH_3C(O)OC(O)CH_2O\cdot \rightarrow HC(O)C(O)\cdot + CH_3C(O)OH \quad (21)$$

As the presence of acetic acid was corroborated by the spectra shown in Figure 3, the temporal variation of the relative percentage analyzed in Figure 5 shows that this acid is a primary photo-oxidation product (32%). In addition, CO and CO_2 could be formed as result of reactions derived from $HC(O)C(O)\cdot$ radical. (Orlando and Tyndall, 2001)

Via D

The intramolecular cyclization is the ultimate pathway resulting from $CH_3C(O)OC(O)CH_2O\cdot$. Scheme 1 presents the complete sequence that can occur for the formation of cyclic anhydride by two alternative routes. On the one hand, abstraction of an H from the $CH_3C(O)OC(O)CH_2O\cdot$ radical by reaction with an oxygen molecule leads to the formation of $HC(O)C(O)OC(O)CH_2OH$, hereafter referred to as "tricarboxylic alcohol". On the other hand, an alternative pathway for the formation of tricarboxylic alcohol involves an isomerization by 1,6 H-migration giving rise to a new radical, where the electron deficiency is supported at the carbon α to the hydroxyl group, as proposed by Aranda et al. (2021 and 2024) and Colmenar et al. (2020) for similar radicals. This

isomer reacts with molecular oxygen to give the tricarboxylic alcohol. Whichever way this alcohol is obtained, this alcohol evolves by intramolecular attack leading to the unstable cyclic anhydride (3-hydroxy-1,4-dioxane-2,6-dione). As shown in Figure 4, it was possible to identify this product, as well as its decomposition products resulting from the heterogeneous reactions (HC(O)OH and CO_2), which were observed in darkness experiments after the photo-oxidation was stopped.

As acetic acid is formed only from *via C*, and formic acid comes only from *via D*, they were used to quantify these paths, yielding 32 % and 20 %, respectively. *Vias A* and *B* share the same end products, so their relative importance cannot be quantified.

In summary, all pathways are available for the $CH_3C(O)OC(O)CH_2O\cdot$ radical. As can be seen, all of them are energetically feasible and the corresponding products were experimentally detected, confirming their occurrence. Since no information on similar radicals is available in the literature, it is not possible to compare the occurrence of these routes for these types of similar radicals. For example, the reactivity of the R-$OC(O)CH_2O\cdot$ radical has not been studied, probably as a consequence of its formation in the photo-oxidation of acetates, its precursor molecule, being in the minority (e.g. Cavalli et al., 2000; Picquet-Varrault et al., 2001). Information is only available on the reactivity of the $CH_3C(O)CH_2O\cdot$ radical, whose structure differs considerably from that corresponding to the radical under study, demonstrating the importance of studies such as the one presented here.

4 Atmospheric implications

From the rate coefficients determined in this work ($k_{Ac2O+Cl}$ and $k_{Ac2O+OH}$) and the average of the concentrations of HO· radicals and Cl atoms available in the literature, the atmospheric lifetime for Ac_2O was calculated from the following relationships:

$$\tau_{OH} = \frac{1}{k_{OH} \times [OH]} \quad \text{(Equation 4)}$$

$$\tau_{Cl} = \frac{1}{k_{Cl} \times [Cl]} \quad \text{(Equation 5)}$$

The reported HO· radical concentration is 2.0×10^6 radicals cm^{-3} (Hein et al., 1997) while chlorine atoms global concentration is 3.3×10^4 atoms cm^{-3}.(Wingenter et al., 1996) Taking these values and determined $k_{Ac2O+Cl}$ and $k_{Ac2O+OH}$ from this study, a τ_{OH} = 31 days and τ_{Cl} = 220 days were derived.

On the other hand, taking into account the presence of carbonyl groups in the structure of the molecule, the atmospheric lifetime as a consequence of wet deposition (τ_{wet}) was calculated according to equation 6 (Chen et al., 2003):

$$\tau_{wet} = \frac{H_{atm} \times H_{Henry}}{J \times R \times T} \quad \text{(Equation 6)}$$

where H_{atm} is assumed to be 6 km (considering that the amount of air in the troposphere is equivalent to that in 6 km of air at 1 atm of pressure), J is the global average precipitation rate and has a value of 100 cm $year^{-1}$ (Warneck, 2000); R = 8.314 Pa m^3 mol^{-1} K^{-1}; T = 275 K correspond to the average tropospheric temperature, and H_{Henry} correspond to the Henry constant for acetic anhydride 0.579 Pa m^{-3} mol^{-1} (Chen et al., 2003; Environment and Climate Change Canada, 2017). From these parameters a τ_{wet} = 1.5 year is obtained for Ac_2O. As can be noted after comparing the lifetimes, it is clear to conclude that the atmospheric degradation of Ac_2O is governed by its reaction with OH· radical leading to the formation of CO, CO_2, $CH_3C(O)OH$ (32 %), $CH_3C(O)OC(O)C(O)H$, and 3-hydroxy-1,4-dioxane-2,6-dione.

Acknowledgements

The authors would like to thank the following funding sources: SECyT-Universidad Nacional de Córdoba (Grant code: 33620180101065CB) and CONICET (Grant code: 11220150100429CO). This work used Mendieta Cluster from CCAD UNC, which is part of SNCAD-MinCyT, Argentina.

References

Akao, M., Saito, K., Oksda, K., Takahashi, O., Tabayashi, K., 1996. Thermal Decomposition of Acetic Anhydride in the Gas Pinase. Physical Chemistry Chemical Physics 100, 1237–1241.

Atkinson, R., 2007. Gas-phase tropospheric chemistry of organic compounds: a review. Atmos Environ 41, 200–240. https://doi.org/10.1016/j.atmosenv.2007.10.068

Atkinson, R., 1997. Gas-Phase Tropospheric Chemistry of Volatile Organic Compounds: 1. Alkanes and Alkenes. J Phys Chem Ref Data 26, 215–290. https://doi.org/10.1063/1.556012

499 Atkinson, R., 1987. A structure-activity relationship for the estimation of rate constants for the
500 gas-phase reactions of OH radicals with organic compounds. Int J Chem Kinet 19, 799–
501 828. https://doi.org/10.1002/kin.550190903

502 Atkinson, R., 1986. Kinetics and mechanisms of the gas-phase reactions of the hydroxyl radical
503 with organic compounds under atmospheric conditions. Chem Rev 86, 69–201.
504 https://doi.org/10.1021/cr00071a004

505 Calvert, J.G., Mellouki, A., Orlando, J.J., Pilling, M.J., Wallington, T.J., 2011. Mechanisms of
506 atmospheric oxidation of the oxygenates. Oxford University Press.

507 Cavalli, F., Barnes, I., Becker, K.H., Wallington, T.J., 2000. Atmospheric oxidation mechanism of
508 methyl propionate. Journal of Physical Chemistry A 104, 11310–11317.
509 https://doi.org/10.1021/jp001702d

510 Chang, C.T., Liu, T.H., Jeng, F.T., 2004. Atmospheric concentrations of the Cl atom, ClO radical,
511 and HO radical in the coastal marine boundary layer. Environ Res 94, 67–74.
512 https://doi.org/10.1016/J.ENVRES.2003.07.008

513 Chemanalyst, 2023. Acetic Anhydride Market Anlysis [WWW Document]. URL
514 https://www.chemanalyst.com/industry-report/acetic-anhydride-market-757

515 Chemical Economics Handbook. S&P Global, 2023. Acetic Anhydride.

516 Chen, L., Takenaka, N., Bandow, H., Maeda, Y., 2003. Henry's law constants for C2-C3
517 fluorinated alcohols and their wet deposition in the atmosphere. Atmos Environ 37,
518 4817–4822. https://doi.org/10.1016/j.atmosenv.2003.08.002

519 Cook, S., 1993. Acetic anhydride, in: Agreda, V., Zoeller, J. (Eds.), Acetic Acid and Its Derivatives.
520 Marcel Dekker, Inc.,New York, NY, pp. 145–161.

521 Environment and Climate Change Canada, 2017. Screening Assessment. Acetic acid, anhydride
522 (acetic anhydride).

523 Frisch, M.J., Trucks, G.W., Schlegel, H.B., Scuseria, G.E., Robb, M.A., Cheeseman, J.R., Scalmani,
524 G., Barone, V., Petersson, G.A., Nakatsuji, H., Li, X., Caricato, M., Marenich, A., Bloino, J.,
525 Janesko, B.G., Gomperts, R., Mennucci, B., Hratchian, H.P., Ortiz, J. V., Izmaylov, A.F.,
526 Sonnenberg, J.L., Williams-Young, D., Ding, F., Lipparini, F., Egidi, F., Goings, J., Peng, B.,
527 Petrone, A., Henderson, T., Ranasinghe, D., Zakrzewski, V.G., Gao, J., Rega, N., Zheng, G.,
528 Liang, W., Hada, M., Ehara, M., Toyota, K., Fukuda, R., Hasegawa, J., Ishida, M., Nakajima,
529 T., Honda, Y., Kitao, O., Nakai, H., Vreven, T., Throssell, K., Montgomery, J.A., Peralta Jr.,
530 J.E., Ogliaro, F., Bearpark, M., Heyd, J.J., Brothers, E., Kudin, K.N., Staroverov, V.N., Keith,
531 T., Kobayashi, R., Normand, J., Raghavachari, K., Rendell, A., Burant, J.C., Iyengar, S.S.,
532 Tomasi, J., Cossi, M., Millam, J.M., Klene, M., Adamo, C., Cammi, R., Ochterski, J.W.,
533 Martin, R.L., Morokuma, K., Farkas, O., Foresman, J.B., Fox, D.J., 2009. Gaussian 09,
534 Revision E.01. Gaussian, Inc., Wallingford CT.

535 Fritzler, B.C., Dharmavaram, S., Hartrim, R.T., Diffendall, G.F., 2014. Acetic Anhydride Hydrolysis
536 at High Acetic Anhydride to Water Ratios. Int J Chem Kinet 46, 151–160.
537 https://doi.org/10.1002/KIN.20838

Hein, R., Crutzen, P.J., Heimann, M., 1997. An inverse modeling approach to investigate the global atmospheric methane cycle. Global Biogeochem Cycles 11, 43–76. https://doi.org/10.1029/96GB03043

Hirota, W.H., Rodrigues, R.B., Sayer, C., Giudici, R., 2010. Hydrolysis of acetic anhydride: Non-adiabatic calorimetric determination of kinetics and heat exchange. Chem Eng Sci 65, 3849–3858. https://doi.org/10.1016/j.ces.2010.03.028

Knopp, J.A., Linnell, W.S., Child, W.C., 1962. The thermodynamics of the thermal decomposition of acetic acid in the liquid phase. Journal of Physical Chemistry 66, 1513–1516. https://doi.org/10.1021/J100814A031/ASSET/J100814A031.FP.PNG_V03

Kwok, E.S.C., Atkinson, R., 1995. Estimation of Hydroxyl Radical Reaction Rate Constants for Gas-Phase Organic Compounds Using a Structure-Reactivity Relationship: An Update. Atmos Environ 29, 1685–1695. https://doi.org/10.1016/1352-2310(95)00069-B

Lewis, M., 1997. Acetic Anhydride, SIDS Initial Assessment Report. Paris.

Mai, T.V.T., Duong, M. V., Nguyen, H.T., Lin, K.C., Huynh, L.K., 2017. Kinetics of thermal unimolecular decomposition of acetic anhydride: an integrated deterministic and stochastic model. Journal of Physical Chemistry A 121, 3028–3036. https://doi.org/10.1021/acs.jpca.7b00015

Notario, A., Le Bras, G., Mellouki, A., LeBras, G., Mellouki, A., 1998. Absolute rate constants for the reactions of Cl atoms with a seies of esters. Journal of Physical Chemistry A 102, 3112–3117.

Orlando, J.J., Tyndall, G.S., 2001. Atmospheric chemistry of the HC(O)CO radical. Int J Chem Kinet 33, 149–156. https://doi.org/10.1002/1097-4601(200103)33:3<149::AID-KIN1008>3.0.CO;2-1

Orlando, J.J., Tyndall, G.S., Wallington, T.J., 2003. The Atmospheric Chemistry of Alkoxy Radicals. Chem Rev 103, 4657–4689. https://doi.org/10.1021/cr020527p

Park, J.Y., Lee, I.H., 2009. Decomposition of acetic acid by advanced oxidation processes. Korean Journal of Chemical Engineering 26, 387–391. https://doi.org/10.1007/S11814-009-0065-2/METRICS

Picquet-Varrault, B., Doussin, J.F., Durand-Jolibois, R., Carlier, P., 2001. FTIR spectroscopic study of the OH-induced oxidation of two linear acetates: Ethyl and n-propyl acetates. Physical Chemistry Chemical Physics 3, 2595–2606. https://doi.org/10.1039/b101704g

Rimondino, G.N., Iriarte, A.G., Grosso, M., Malanca, F.E., 2021. Kinetic and mechanistic studies of atmospheric degradation of diethyl pyrocarbonate initiated by OH radicals and chlorine atoms. J Photochem Photobiol A Chem 418, 113409–113416. https://doi.org/10.1016/j.jphotochem.2021.113409

Rimondino, G.N., Iriarte, A.G., Malanca, F.E., 2023. Photo-oxidation of ethyl pyruvate initiated by chlorine atoms. Kinetics and reaction mechanism. J Photochem Photobiol A Chem 440, 114655–114662. https://doi.org/10.1016/j.jphotochem.2023.114655

Rimondino, G.N., Peláez, W.J., Malanca, F.E., 2020. Atmospheric Photo-oxidation of Diethyl Carbonate: Kinetics, Products, and Reaction Mechanism. Journal of Physical Chemistry A 124, 56–62. https://doi.org/10.1021/acs.jpca.9b09887

579 Scollard, D.J., Treacy, J.J., Sidebottom, H.W., Balestra-Garcia, C., Laverdet, G., LeBras, G.,
580 MacLeod, H., Téton, S., 1993. Rate constants for the reactions of hydroxyl radicals and
581 chlorine atoms with halogenated aldehydes. Journal of Physical Chemistry 97, 4683–4688.
582 https://doi.org/10.1021/J100120A021/ASSET/J100120A021.FP.PNG_V03

583 Straccia C, V.G., Rivela, C.B., Blanco, M.B., Teruel, M.A., 2023. Kinetics and products study of
584 the reaction of Cl atoms with methyl dichloroacetate: reactivity, mechanism, and
585 environmental implications. Environmental Science: Atmospheres 3, 872–881.
586 https://doi.org/10.1039/d3ea00004d

587 Wagner, F.S., 2014. Acetic anhydride, in: Kirk-Othmer Encyclopedia of Chemical Technology.
588 Wiley-VCH Verlag GmbH & Co., pp. 146–160.
589 https://doi.org/10.1002/9780471264194.fos00021.pub3

590 Warneck, P., 2000. Chemistry of the natural atmosphere, Second edi. ed. Elsevier Science.

591 Wingenter, O.W., Kubo, M.K., Blake, N.J., Smith, T.W., Blake, D.R., Rowland, F.S., 1996.
592 Hydrocarbon and halocarbon measurements as photochemical and dynamical indicators
593 of atmospheric hydroxyl, atomic chlorine, and vertical mixing obtained during Lagrangian
594 flights. Journal of Geophysical Research Atmospheres 101, 4331–4340.
595 https://doi.org/10.1029/95JD02457

596 Yoshida, H., Takeda, K., Okamura, J., Ehara, A., Matsuura, H., 2002. A New Approach to
597 Vibrational Analysis of Large Molecules by Density Functional Theory: Wavenumber-
598 Linear Scaling Method. J Phys Chem A 106, 3580–3586.
599 https://doi.org/10.1021/jp013084m

600 Young, C.J., Washenfelder, R.A., Edwards, P.M., Parrish, D.D., Gilman, J.B., Kuster, W.C., Mielke,
601 L.H., Osthoff, H.D., Tsai, C., Pikelnaya, O., Stutz, J., Veres, P.R., Roberts, J.M., Griffith, S.,
602 Dusanter, S., Stevens, P.S., Flynn, J., Grossberg, N., Lefer, B., Holloway, J.S., Peischl, J.,
603 Ryerson, T.B., Atlas, E.L., Blake, D.R., Brown, S.S., 2014. Chlorine as a primary radical:
604 Evaluation of methods to understand its role in initiation of oxidative cycles. Atmos Chem
605 Phys 14, 3427–3440. https://doi.org/10.5194/acp-14-3427-2014

606